



1 **DIURNAL, SEASONAL AND SOLAR CYCLE VARIATION OF TOTAL ELECTRON
2 CONTENT AND COMPARISON WITH IRI-2016 MODEL AT BIRNIN-KEBBI**

3 Aghogho Ogwala,^{1,*}Emmanuel Olufemi Somoye,¹Olugbenga Ogunmodimu.,³Rasaq
4 Adewemimo Adeniji-Adele,¹Eugene Oghenakpobo Onori,¹Oluwole Oyedokun²

5 ^{1,*} Department of Physics, Lagos State University, Lagos, Nigeria.

6 ²Department of Physics, University of Lagos, Nigeria.

7 ³ Department of Electrical Engineering, Manchester Metropolitan University, United Kingdom.

8 **ABSTRACT**

9 Total Electron Content (TEC) is an important ionospheric parameter used to monitor possible
10 space weather impacts on satellite to ground communication and satellite navigation system.
11 TEC is modified in the ionosphere by changing solar Extreme Ultra-Violet (EUV) radiation,
12 geomagnetic storms, and the atmospheric waves that propagate up from the lower atmosphere.
13 Therefore, TEC depends on local time, latitude, longitude, season, geomagnetic conditions, solar
14 cycle activity, and condition of the troposphere. A dual frequency GPS receiver located at an
15 equatorial station, Birnin-Kebbi in Northern Nigeria (geographic location: 12.64°N; 4.22°E), has
16 been used to investigate variation of TEC during the period of 2011 to 2014. We investigate the
17 diurnal, seasonal and solar cycle dependence of observed (OBS) TEC and comparison with latest
18 version of International Reference Ionosphere (IRI-2016) model. On a general note, diurnal
19 variation reveals discrepancies between OBS-TEC and IRI-2016 model for all hours of the day
20 except during the post-midnight hours. Slight post-noon peaks in the daytime maximum and
21 post-sunset decrease and enhancement are observed in the diurnal variation of OBS-TEC of
22 some months. On a seasonal scale, we observed that OBS-TEC values were higher in the



23 equinoxes than the solstices only in 2012. Where as in 2011, September equinox and December
24 solstice recorded higher magnitude followed by March equinox and lowest in June solstice. In
25 2013, December solstice magnitude was highest, followed by the equinoxes and lowest in June
26 solstice. In 2014, March equinox and December solstice magnitude were higher than September
27 equinox and June solstice magnitude. June solstice consistently recorded the lowest values for all
28 the years. OBS-TEC is found to increase from 2011 to 2014, thus revealing solar cycle
29 dependence.

30 **KEYWORDS:** TEC; diurnal; seasonal; variation; solar cycle 24; IRI-2016.

31 **CORRESPONDING AUTHOR PHONE:** +234 8055650264

32 **CORRESPONDING AUTHOR E-MAIL:**ogwala02@gmail.com

33

34

35

36

37

38

39

40

41

42

43

44

45

46

47



48 INTRODUCTION

49 The ionosphere causes a variation in the intensity of radio signals – fading – as a result of
50 irregularities (inhomogeneity in electron density) (Somoye, 2010; Ogwala *et al.* 2018,
51 Ogunmodimu *et al.* 2018). Akala *et al.*, (2011) reported that the variable nature of the equatorial/
52 low latitude ionosphere threatens communication and navigation/ satellite systems. The
53 equatorial/ low latitude ionosphere exhibits many unique features such as the seasonal anomaly,
54 semi-annual anomaly, equinoctial anomaly, noon bite-out, spread-F, equatorial electrojet (EEJ),
55 equatorial plasma bubbles (EPB), etc.

56 For many decades, scientists have been studying these ionospheric features and the role
57 they play in trans-ionospheric electromagnetic radio wave propagation. These studies are carried
58 out using different techniques and instruments. One of the instruments used is the GPS receiver,
59 which provide direct measurements from satellites. Their sounding capacity extends to the
60 topside of the ionosphere, but is affected by time and space constraints (Ciraolo and Spalla,
61 2002). Recently, GPS receiver is the most efficient method used to eliminate the effect of the
62 ionosphere on radio signals. This method combines signals in different L band frequencies, L1
63 (1575 MHz) and L2 (1228 MHz).

64 Almost all space geodetic techniques transmit signals in at least two different frequencies
65 for better accuracy (Alizadeh *et al.*, 2013). These are combined linearly and can greatly eliminate
66 the effect of the ionosphere on radio signals. The ionospheric effect on radio signal is
67 proportional to total electron content (TEC), which is defined as the number of electrons per
68 square meter from satellite in space to receiver on ground is shown in equation (1).

$$69 TEC = \int n_e(s)ds \quad (1)$$



70 It is measured in multiples of TEC units ($1 \text{ TECU} = 10^{16} \text{ el/m}^2$). Due to the dispersive
71 nature of the ionosphere, there is a time delay between the two frequencies of a GNSS signal as
72 it propagates through the ionosphere shown in Equation (2) as $\Delta t = t_2 - t_1$. Thus,

$$73 \Delta t = \left(\frac{40.3}{c} \right) \times \frac{\text{TEC}}{\left[\left(\frac{1}{f_2^2} \right) - \left(\frac{1}{f_1^2} \right) \right]} \quad (2)$$

74 Where c is speed of light and f is frequency. Hence, Δt measured between the L1 and L2
75 frequencies is used to evaluate TEC along the ray path.

76 When Global Navigation Satellite System (GNSS) signals propagate through the
77 ionosphere, the carrier experiences phase advance and the code experiences a group delay due to
78 the electron density along the line of sight (LOS) from the satellite to the receiver (Bagiya *et al.*,
79 2009; Tariku, 2015). Thus, the carrier phase pseudo ranges are measured too short, and the code
80 pseudo ranges are measured too long compared to the geometric range between the satellite and
81 the receiver. This results in a range error of the positioning accuracy provided by a GPS receiver.
82 The range error due to TEC in the ionosphere varies from hundreds of meters at mid-day, during
83 high solar activity when the satellite is near the horizon of the observer, to a few meters at night
84 during low solar activity, with the satellite positioned at zenith angle (Bagiya *et al.*, 2009). By
85 measuring this delay using dual frequency GPS receivers, properties of the ionosphere can be
86 inferred and used to monitor space weather events such as GNSS, HF communications, Space
87 Based Observation Radar and Situational Awareness Radar, etc. It is documented that
88 ionospheric delay which is proportional to TEC is the highest contributor to GPS positioning
89 error (Alizadeh *et al.*, 2013; Akala *et al.*, 2013).

90 TEC in the ionosphere can also be studied using empirical ionospheric model such as the
91 International Reference Ionosphere (IRI). IRI is a joint undertaking by the Committee on Space



92 Research (COSPAR) and International Union of Radio Science (URSI) with the goal of
93 developing and improving an international standard for the parameters in earth's ionosphere
94 (Bilitza *et al.*, 2014). An updated version has been developed recently to cater for lapses of
95 previous models. IRI provides the vertical TEC (VTEC) from the lower boundary (60 – 80 km)
96 to a user-specific upper boundary (Bilitza *et al.*, 2016).

97 In the past few decades, studies on the temporal and spatial variations of TEC have
98 gained popularity in the scientific community (Wu *et al.*, 2008). However, understanding the
99 variability of TEC will also go a long way in obtaining the positioning accuracy of GNSS under
100 disturbed and quiet conditions. The global distribution of TEC variations and its characteristics at
101 all latitudes, during different solar cycle phases under disturbed and quiet conditions have been
102 investigated by some researchers (Bhuyan and Borah, 2007).

103 Rama Rao *et al.* (2006a, b) reported maximum day-to-day variability in TEC at the
104 Equatorial Ionization Anomaly (EIA) crest regions, increasing peak value of TEC with increase
105 in integrated equatorial electrojet (IEEJ) strength, maximum monthly average diurnal variations
106 during equinox months followed by winter months and lowest during summer months. They also
107 reported positive correlation of TEC and EEJ and the spatial variation of TEC in the equatorial
108 region. Titheridge (1974) attributed the lower TEC values during the summer seasons to low
109 ionization density resulting from reduced O/ N₂ ratio (production rates) which is a result of
110 increased scale height. Bhuyan and Borah (2007) compared TEC derived from GPS receivers
111 with IRI in the Indian sector and inferred that the diurnal amplitude of TEC is higher during the
112 equinoxes followed by December solstices and lowest in June solstice, i.e., observing winter
113 anomaly in seasonal variation. Akala *et al.* (2013) on the comparison of equatorial GPS-TEC
114 observations over an African station and an American station during the minimum and ascending



115 phases of solar cycle 24 reported that seasonal VTEC values were maximum and minimum
116 during March equinox and June solstice respectively, during minimum solar cycle phase at both
117 stations. They also reported that during the ascending phase of solar cycle 24, minimum and
118 maximum seasonal VTEC values were recorded during December solstice and June solstice
119 respectively. They further showed that IRI-2007 model predicted better in the American sector
120 than the African sector.

121 In this research, the result obtained in 2012 and 2013 which corresponds to the result of
122 these researchers. However, the result we obtained in 2011 and 2014 did not follow the trend
123 reported by these researchers, who explored the equatorial/ low latitude during different solar
124 cycle epochs. We also observed discrepancies between the OBS-TEC and IRI-2016 almost
125 throughout the day for all the years in this research.

126

127 DATA AND METHODOLOGY

128 2.1 DATA

129 The Receiver Independence Exchange (RINEX) Observation GPS data files were
130 downloaded daily from NIGNET website (www.nignet.net) and processed using Bernese
131 software and GPS TEC analysis software. The RINEX file contains 60 iteration data (i.e. in 1
132 minute time resolution). The GPS-TEC analysis software was designed by Gopi Seemala of the
133 Indian Institute of Geomagnetism. The summary of this application are, reads raw data,
134 processes cycle slips in phase data, reads satellite biases from the International GNSS services
135 (IGS) code files (and calculates them if unavailable), and calculates receiver bias, inter-channel
136 biases for different satellites in the constellation, and finally plots the VTEC values on the screen
137 and writes the ASCII output files (*CMN) for STEC and (*STD) for VTEC in the same directory



138 of the data files. Effect due to multipath is eliminated by using a minimum elevation angle of
139 50°.

140 Observation GPS-TEC obtained from the TEC analysis software is the slant TEC (STEC)
141 and vertical TEC (VTEC). STEC is polluted with several biases that must be eliminated to get
142 VTEC. VTEC is calculated from the daily values of STEC using equation (3).

143
$$VTEC = (STEC - [b_R + b_S + b_{RX}])/S(E) \quad (3)$$

144 Where b_R , b_S , and b_{RX} are receiver bias, satellite bias receiver interchannel bias respectively.
145 $S(E)$, which is the oblique factor with zenith angle, z at IPP (Ionospheric Pierce Point) is
146 expressed in equation (4).

147
$$S(E) = \frac{1}{\cos(z)} = \left\{ 1 - \left(\frac{R_E \times \cos(E)}{R_E + h_S} \right)^2 \right\}^{-0.5} \quad (4)$$

148 R_E = the mean radius of the earth in km and h_S = ionospheric height from the surface of the earth.
149 According to Rama Rao *et al.*, (2006c), ionospheric shell height of approximately 350km is
150 appropriate for the equatorial/ low latitude region of the ionosphere for elevation cut off angle of
151 $> 50^\circ$. This is valid in this study.

152 Hourly VTEC data obtained from these processing software are averaged to daily TEC
153 values in TEC units (1 TECU = 10^{16} el/m²). OBS-TEC from Birnin-kebbi, on geographic
154 Latitude 12.47°N and geographic Longitude 4.23°E located in Northern Nigeria, obtained during
155 the period 2011 – 2014, which corresponds to the ascending (2011 – 2013) and maximum (2014)
156 phases of solar cycle 24 were compared with derived TEC obtained from International Reference
157 Ionosphere (IRI-2016) model website
158 (https://ccmc.gsfc.nasa.gov/modelweb/models/iri2016_vitmo.php). The 2016 version of IRI
159 provides important changes and improvements on previous IRI versions (Bilitza *et al.*, 2016).
160 Solar cycle 24 is regarded as a quiet solar cycle which peaked in 2014 with maximum sunspot



161 number (103) occurring in February. Values of sunspot number, Rz, in Text format were
162 obtained from Space Physics Interactive Data Resource (SPIDR) website
163 (www.ionosonde.spidr.com) before it became unavailable. Table 1 shows the years used in this
164 study and their corresponding sunspot number, Rz.

165

166 Table I: Table of years, solar cycle phase and sunspot number, Rz [Source: Author].

Years	Solar Cycle Phase	Sunspot Number, Rz
2011	Ascending	55.7
2012	Ascending	57.6
2013	Ascending	64.7
2014	Maximum	79.6

167

168

169 2.2 METHODOLOGY

170 Comparison of diurnal variations of OBS-TEC with error bars and IRI-2016 (NeQuick
171 topside option) model, and their corresponding percentage deviation (percentage Dev or % DEV)
172 were analysed using the monthly mean values of VTEC with respect to local time (LT). % DEV
173 was obtained using equations (5) below:

$$174 \%DEV = \left(\frac{OBS - IRI}{OBS} \right) \times 100 \quad (5)$$

175 where OBS represents Observation-TEC values and IRI represents TEC derived by IRI-2016.

176 The annual variation of OBS-TEC and IRI-2016 model were plotted against all hours
177 from the first day of January to the last day of December for the years under investigation (2011
178 – 2014). The OBS-TEC data was grouped following Onwumechilli and Ogbuehi (1964) into four



179 seasons namely: March equinox (February, March and April), June solstice (May, June and
180 July), September equinox (August, September and October) and December solstice (November,
181 December and January), in order to investigate seasonal variation. Finally, Annual variation of
182 OBS-TEC and sunspot number, Rz were also analysed by plotting mean TEC and mean Rz
183 against each month of the year.

184 **RESULT AND DISCUSSIONS**

185 Figures 1 to 4 shows the diurnal variation of OBS-TEC in the Nigerian Equatorial
186 Ionosphere (NEI) for the years 2011 to 2014 respectively, were represented by data obtained
187 from the GPS receiver installed at Birnin-Kebbi station and IRI-2016 model. The diurnal
188 variation of OBS-TEC reveals the typical characteristics of an equatorial/ low latitude
189 ionosphere. Generally, top and bottom error bar is used to show day-to-day TEC variation. The
190 study reveal day-to-day variation of TEC is higher during the daytime than night time for all the
191 years. The diurnal variation shows OBS-TEC rising rapidly from a minimum just before sunrise
192 between 03:00 – 05:00 LT (~2 TECU) in 2011, 04:00 – 05 LT (~3 TECU) in 2012, 03:00 –
193 05:00 LT in 2013 (~3 TECU), and 03:00 – 05:00 LT in 2014 (~3 TECU). OBS-TEC is found to
194 increase to a broad daytime maximum between 00:12 LT – 00:16 LT for all years before falling
195 to a minimum after sunset. The diurnal variation of IRI-2016 model shows TEC rising from a
196 minimum of ~ 2 TECU in 2011, ~ 4 TECU in 2012 and 2013, and ~ 5 TECU in 2014 between
197 03:00 – 04:00hr, to a broad daytime peak between 08:00 – 14:00hr, before falling steeply to
198 minimum before sunset. Hence the IRI-2016 model attained its peak before OBS-TEC. The steep
199 increase in TEC has been attributed to the solar EUV ionization together with the upward
200 vertical $E \times B$ resulting from the rapid filling up of the magnetic field tube at sunrise (Dabas *et
al.*, 2003; Somoye *et al.*, 2011; Hajra *et al.* 2016; D'ujanga *et al.*, 2017) and meridional winds



202 (Suranya *et al.*, 2015). These magnetic field tubes collapse after sunset due to low thermospheric
203 temperature and Releigh Taylor Instability (RTI) (Ayorinde *et al.*, 2016) giving rise to the
204 minimum TEC values after sunset. These results are similar to findings of Bolaji *et al.*, (2012),
205 Fayose *et al.*, (2012), Okoh *et al.*, (2014), Eyelade *et al.*, (2017) who have explored the NEI.

206

207

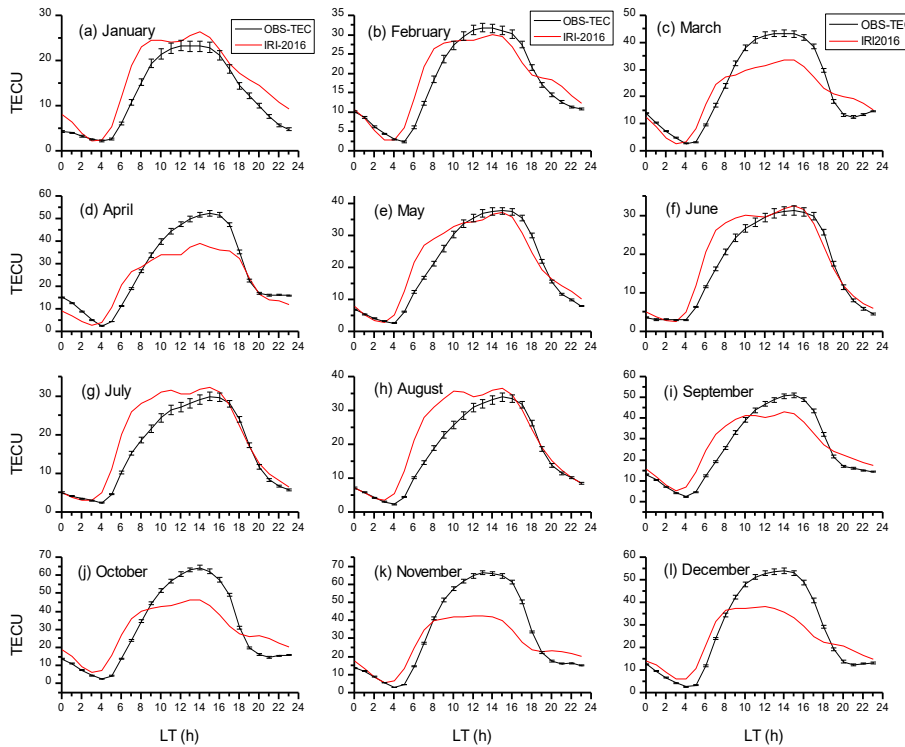


Figure 1: Diurnal variation of OBS-TEC and IRI-2016 model of each month during January – December 2011 at Birnin-Kebbi

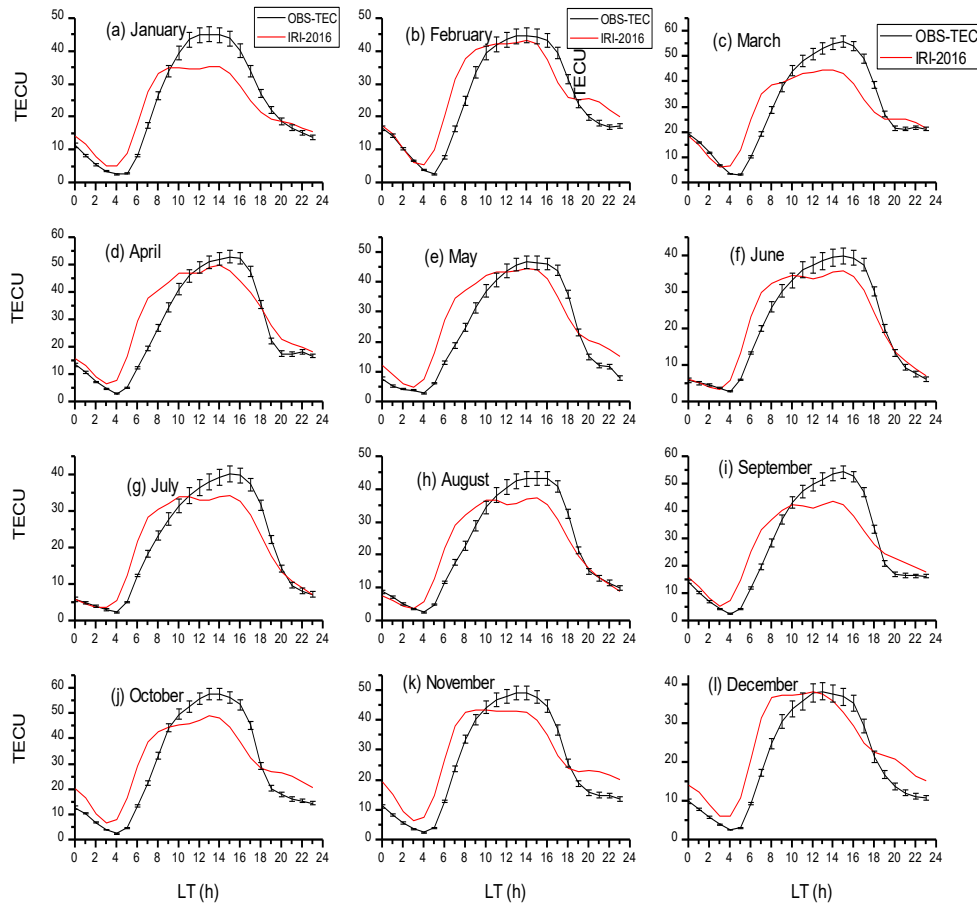
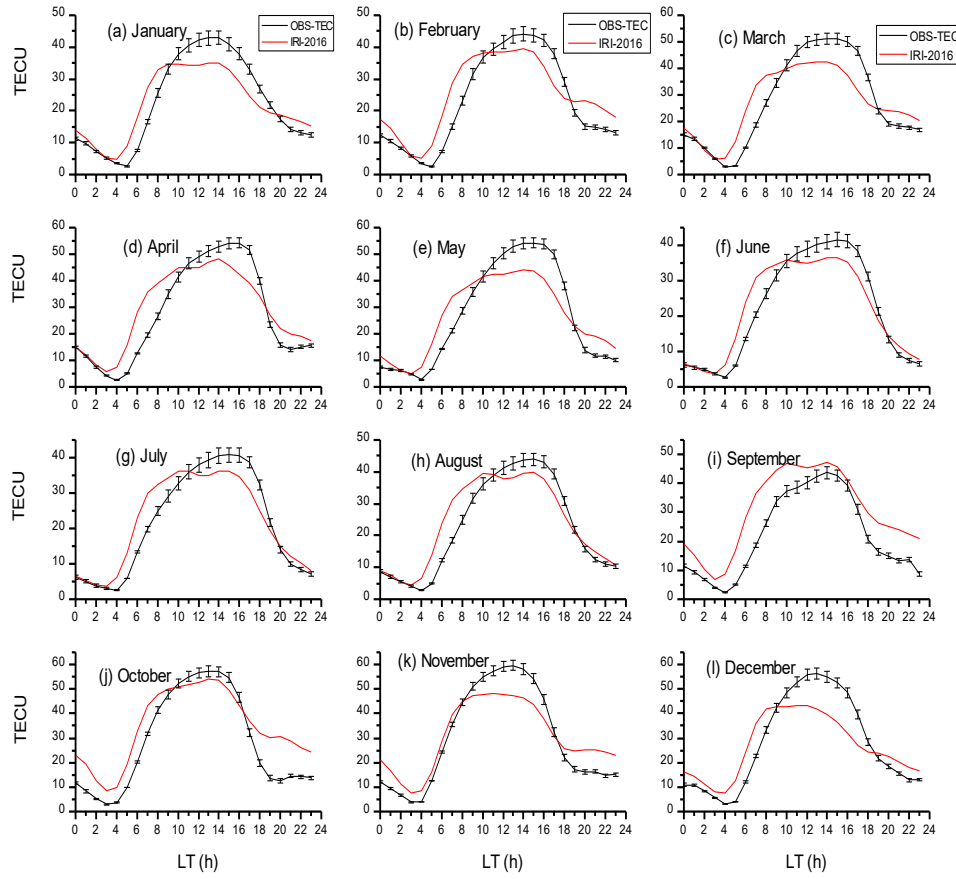


Figure 2: Diurnal variation of OBS-TEC and IRI-2016 model of each month during January – December 2012 at Birnin-Kebbi

219

220



221
222

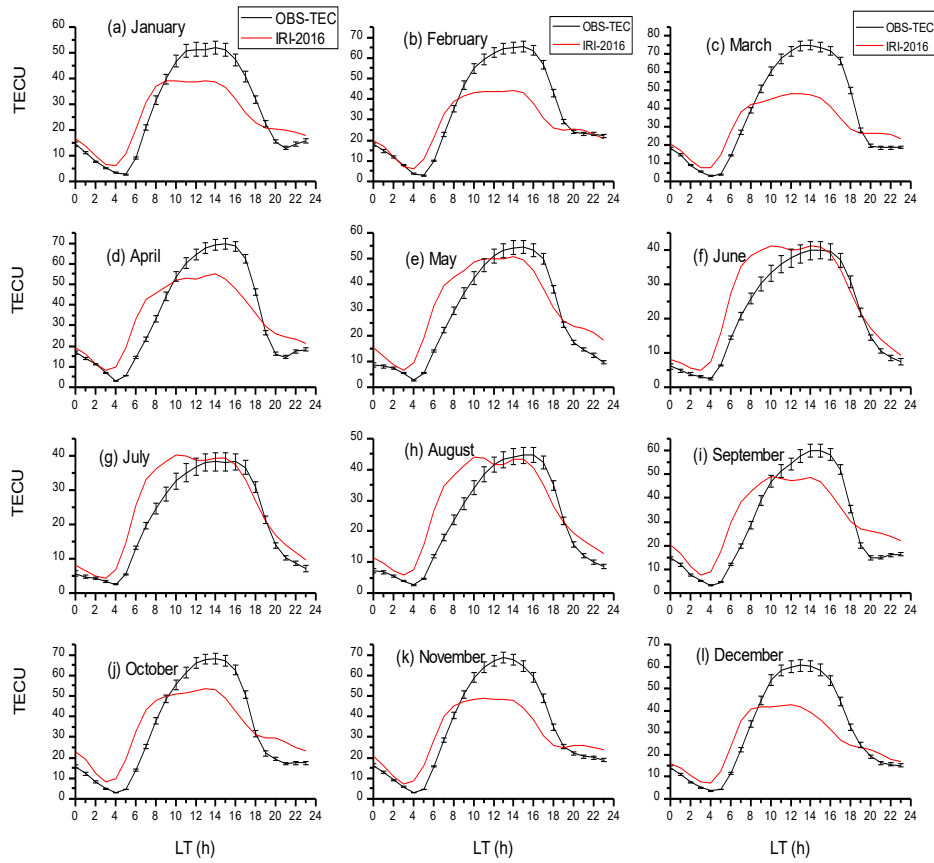
Figure 3: Diurnal variation of OBS-TEC and IRI-2016 model of each month during January – December 2013 at Birnin-Kebbi

223

224

225

226



227 Figure 4: Diurnal variation of OBS-TEC and IRI-2016 of each month during January – December
228 2014 at Birnin-Kebbi

229 It can be seen that OBS-TEC is much higher in 2014 with maximum values up to 70
230 TECU in March compared with IRI-2016 maximum of 54 TECU in the month of October, 2014.
231 The diurnal variation reveals that the peak of OBS-TEC of some months was delayed till after
232 noon. For example, the months of April, July, August and September in 2011, March, April, June
233 and September in 2012, April, June, July and September in 2013 had delayed peak. The delayed
234 OBS-TEC peaks were also seen in April, May, June, August and September of 2014. This type



235 of peak shifting is peculiar to the Polar Regions and it is found to depend on the solar zenith
236 angle. Another major phenomenon seen in the diurnal variation of OBS-TEC is the post-sunset
237 decrease and slight enhancement in some months. The night time enhancement of TEC, for
238 example, March, April and October of the year 2011, March and April of the year 2012, March,
239 April, September and October of the year 2013, January, April and September of the year 2014
240 was documented by previous researchers like Rama Rao *et al.*, 2009; D'ujanga *et al.*, 2017. They
241 attributed it to the product of eastward and westward directed electric field which produces an
242 upward and downward motion of ionospheric plasma during the day and night respectively.

243 Figures 5 to 8 shows the diurnal variation of percentage deviation of IRI-2016 model
244 from OBS-TEC in the Nigerian Equatorial Ionosphere (NEI) for all years respectively. On a
245 general note, IRI-2016 model only presented suitable predictions for the post-midnight hour
246 between 00 – 04hr of the day for all years. All other hours from 05 – 23hr shows some
247 discrepancies. In some months, these discrepancies lasted throughout the day for example, in the
248 months of October, November and December of 2012, October and December, 2013, and
249 September and October of 2014, while in some other months these discrepancies collapsed
250 during the pre-midnight hours, for example, in the months of June, July and August of 2011,
251 June, July and August of 2012, June and August of 2013 and February, June and July of 2014. It
252 is also important to mention that IRI-2016 model either over estimated or under estimated TEC
253 in the NEI especially during daytime hours as shown in plots.

254
255

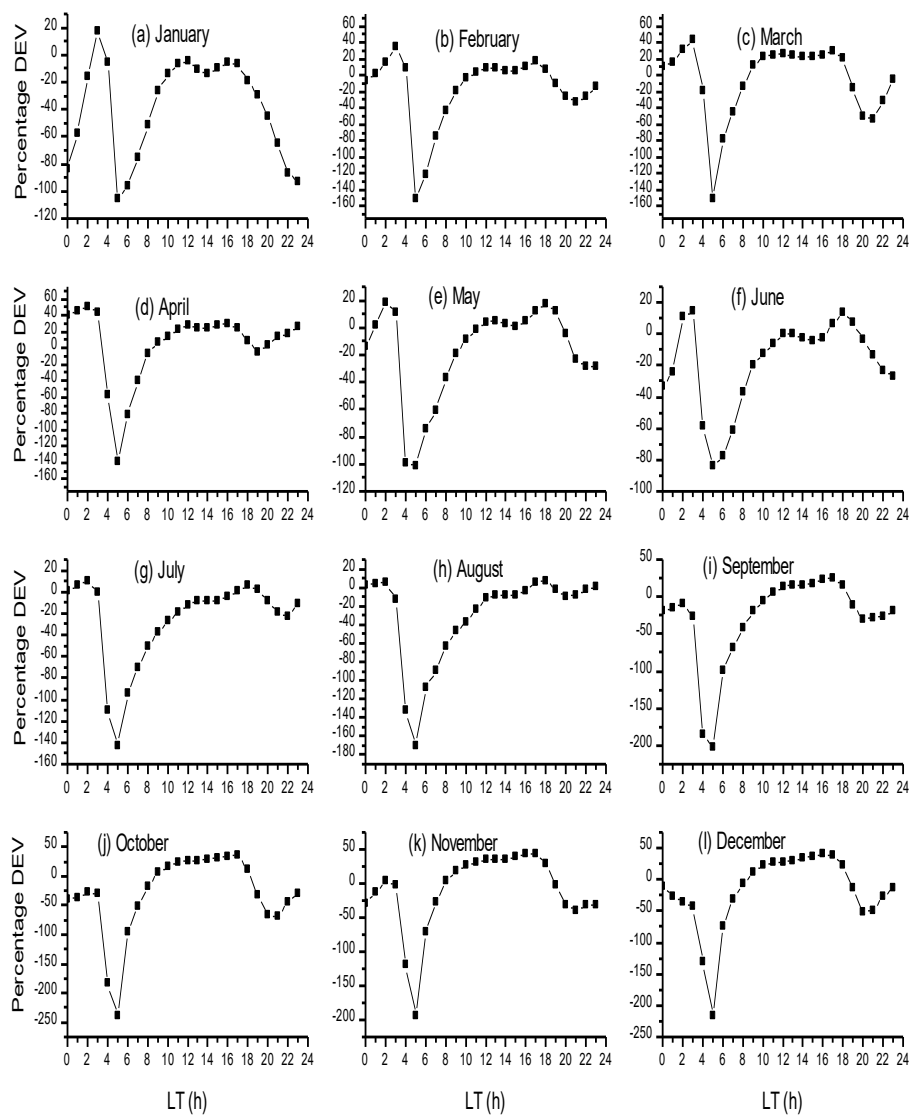
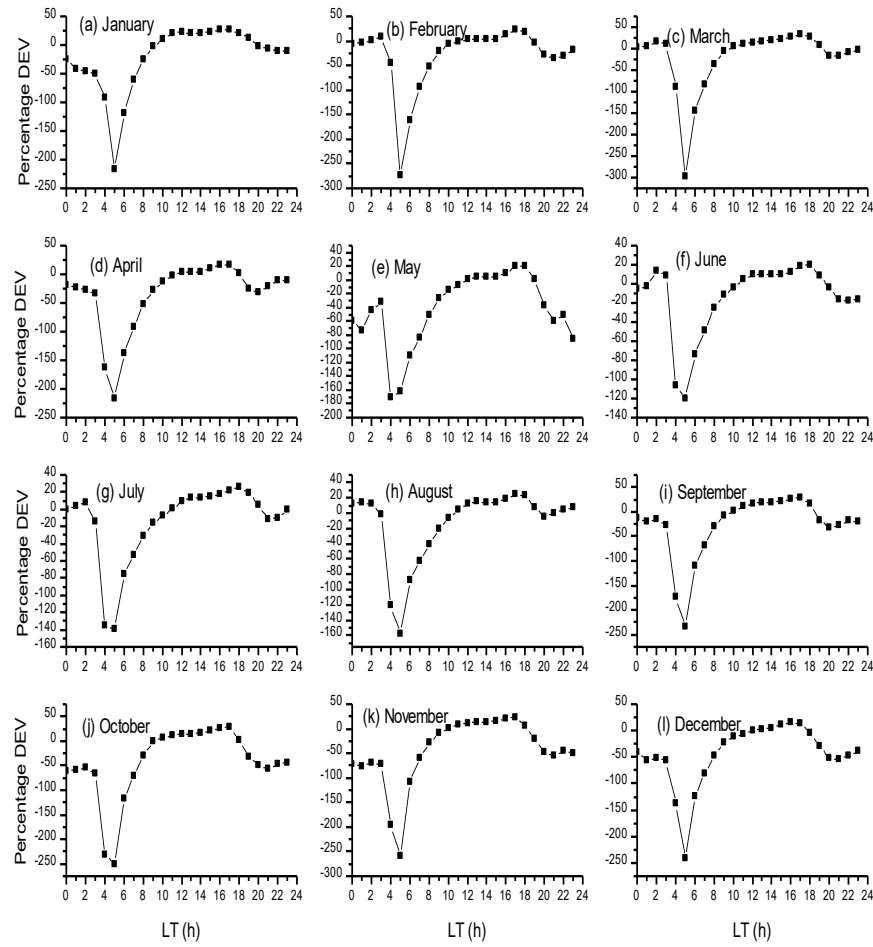


Figure 5: Percentage deviation of IRI-2016 from OBS-TEC for year 2011



258

Figure 6: Percentage deviation of IRI-2016 from OBS-TEC for year 2012

259

260

261

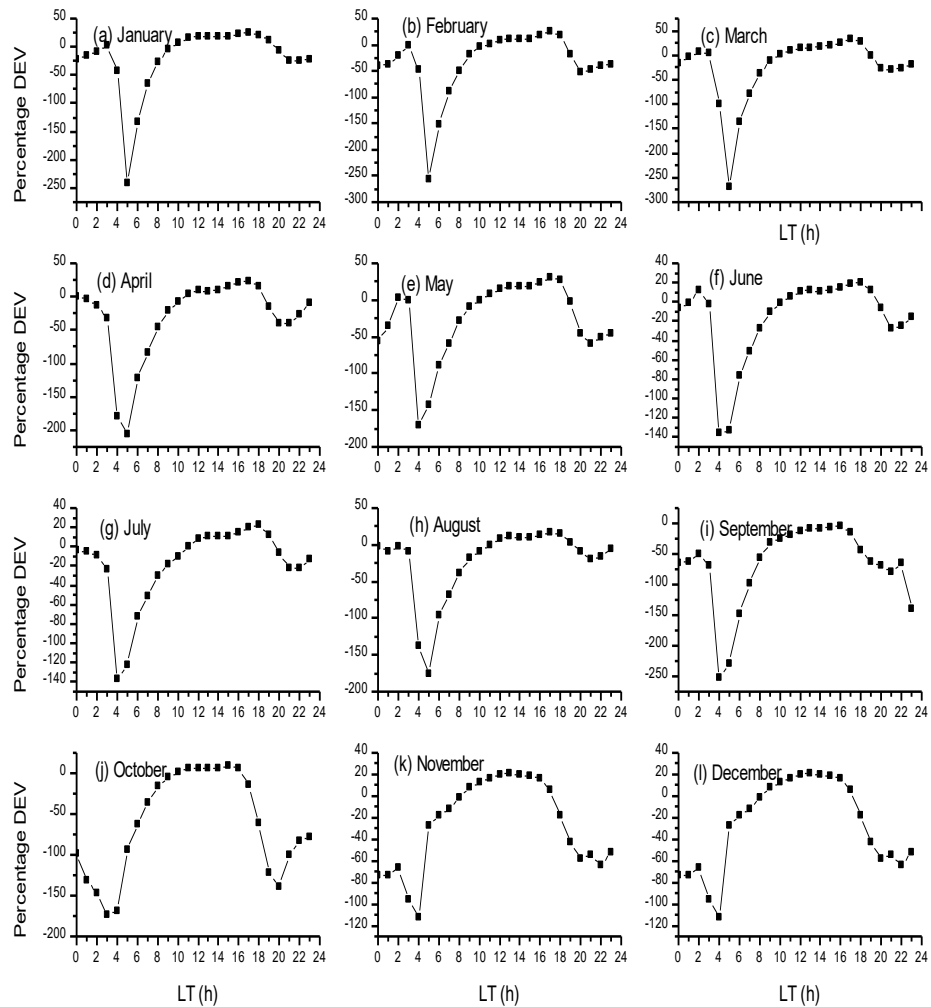


Figure 7: Percentage deviation of IRI-2016 from OBS-TEC for year 2013

262

263

264

265

266

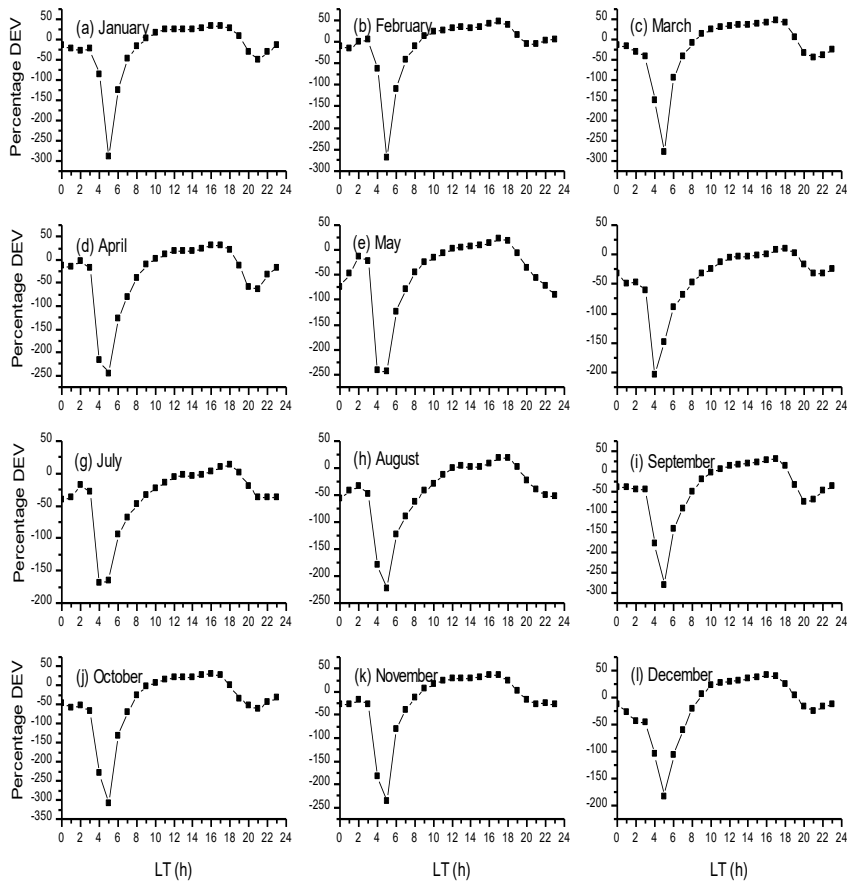


Figure 8: Percentage deviation of IRI-2016 from OBS-TEC for year 2014

267

268 The mass plots in the Figures 5 - 8 further reveal that negative percentage deviation
 269 shows higher values of IRI-2016 than OBS-TEC values. The reverse is the case for positive
 270 percentage deviation. Highest negative percentage deviations are seen between 04 – 05hr for all
 271 months throughout the years in this study. Highest Negative percentage deviation of ~ 300% was
 272 recorded in the month of October, 2014 at 05hr. Table II shows the summary of months with
 273 daytime over- or under-estimate of IRI-2016 in the NEI.



274

Table II: Months of daytime estimate of IRI-2016 model in NEI [Source: Author]

YEAR	OVER ESTIMATE	UNDER ESTIMATE	SAME RANGE
2011	January, July, August	February – April, September – December	May - June
2012		January - December	
2013	September	January – August, October – December	
2014		January - December	

275

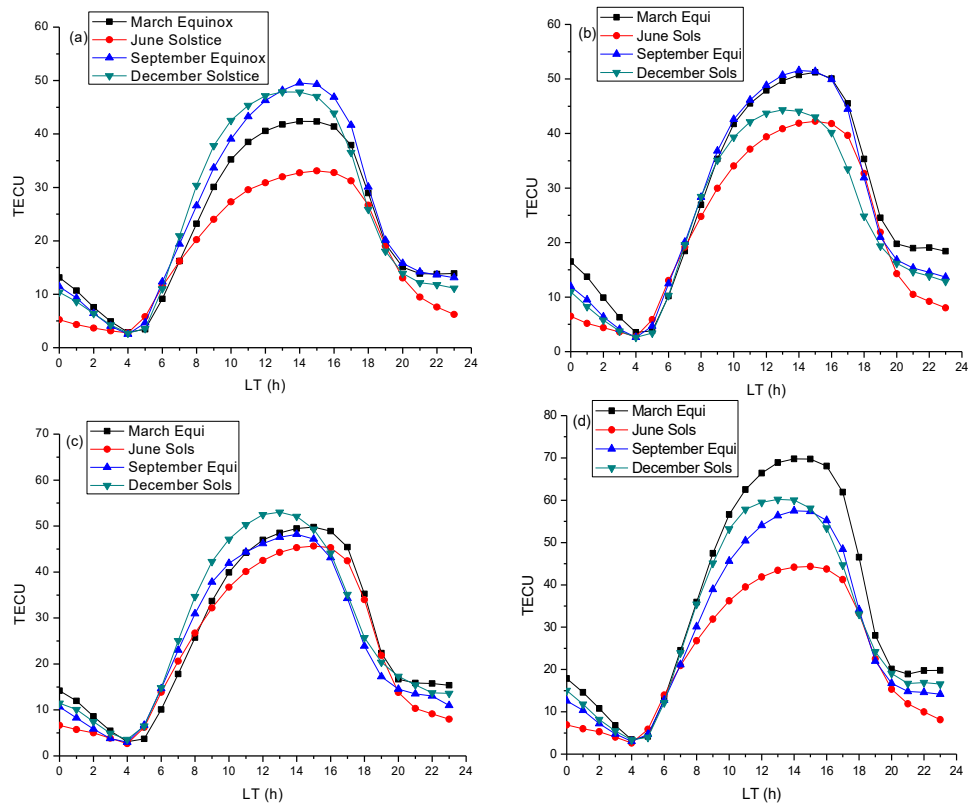
276 Therefore, it is clear from the Figures 1- 4, Figures 5 – 8 and Table II that IRI-2016
277 model did not predict well in the NEI. This could be attributed to the scarce GPS infrastructure
278 and data in the region.

279 Figure 9 plots the seasonal variations of OBS-TEC for the four years under investigation.
280 The change in concentration of Oxygen and molecular Nitrogen has been reported to be the main
281 cause of seasonal variation of ionospheric parameters. Seasonal variation of OBS-TEC in this
282 study depicts semi-annual variation with equinoctial maximum (~ 52 TECU) and solsticial
283 minimum (~ 44 TECU) in 2012. D'ujanga *et al.*, (2017) reported that since the sun passes
284 through the equator during the equinox, both March and September equinox experience the same
285 solar radiation. It is also a well-established fact that March 20 and September 23 are the only
286 times in the year when the solar terminator is perpendicular to the equator, giving rise to the
287 equinoctial maximum. The semi-annual variation has been attributed to the effect of solar zenith
288 angle and magnetic field geometry (Wu *et al.*, 2004; Rama Rao *et al.*, 2006a). Another important
289 feature of ionospheric parameters (known as equinoctial asymmetry) which is reported in the



290 work of Bolaji *et al.*, (2012); Akala *et al.*, (2013); Eyelade *et al.*, (2017); D'ujanga *et al.*, (2017);
 291 Aggarwal *et al.*, (2017), is clearly seen in all years used in this work. Akala *et al.*, (2013) also
 292 reported minimum and maximum seasonal VTEC values during December solstice and June
 293 solstice respectively, during ascending phase of solar cycle 24. Equinoctial asymmetry is a
 294 strong phenomenon in low latitudes (Aggarwal *et al.*, 2017). The equinoctial asymmetry has
 295 been explained in terms of the differences in the meridional winds leading to changes in the
 296 neutral gas composition during the equinoxes.

297



298

299 Figure 9: Seasonal variation of observed OBS-TEC during (a) 2011 (b) 2012 (c) 2013 and
 (d) 2014

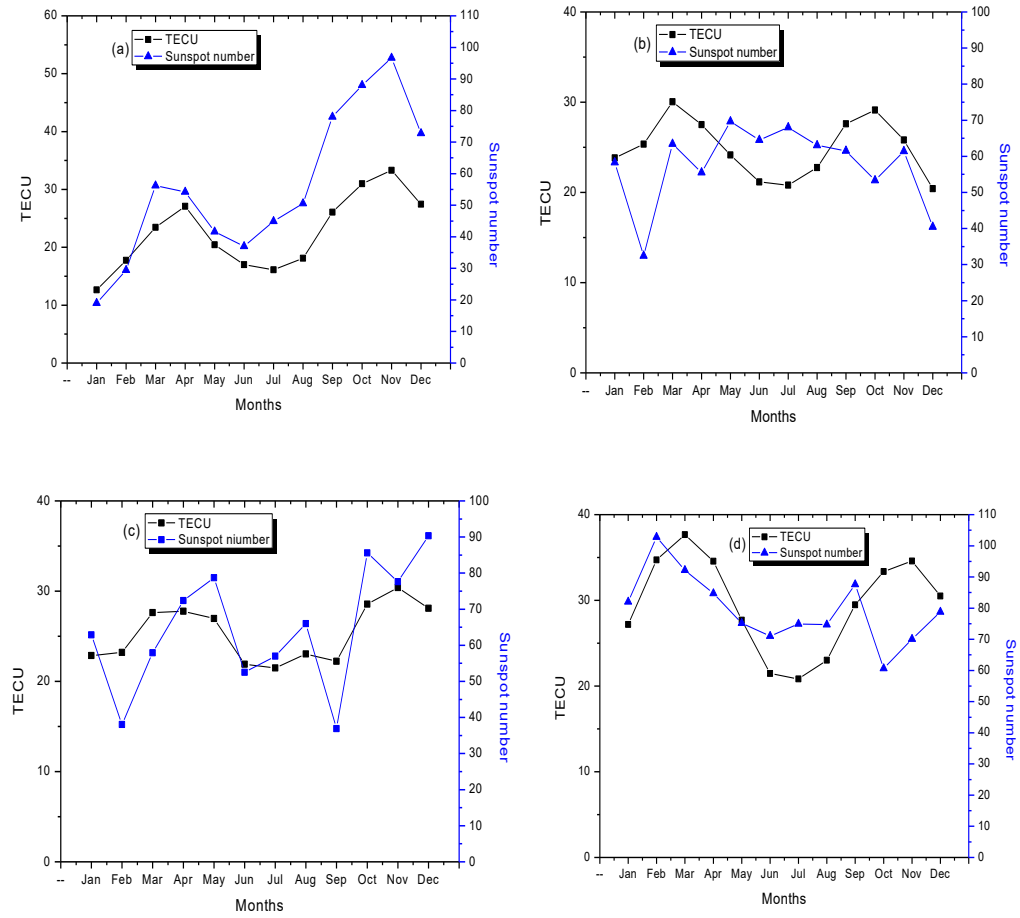


300 In 2011 and 2014, the seasonal variation of OBS-TEC in the ionosphere did not follow
301 the pattern reported by these researchers. In 2011, September equinox and December solstice
302 recorded higher magnitude, followed by March equinox; the lowest was in June solstice. In
303 2013, December solstice magnitude was highest, followed by the equinoxes, March and
304 September respectively and lowest in June solstice. This corresponds to result obtained by Akala
305 *et al.* (2013), which they attributed to increase in ion production rate in winter season and anti-
306 correlation between December and June Solstice pre-reversal velocity enhancement. In 2014,
307 March equinox and December solstice magnitudes were higher than September equinox and June
308 solstice magnitudes. December solstice magnitude is found to occur between the magnitudes of
309 the equinoxes in 2011 and 2014. The September equinox magnitude and March equinox
310 magnitude are observed to interchange in 2011 and 2014. Overall, June solstice magnitudes were
311 lowest during all the years. This is due to low ionization resulting from reduced production rates,
312 i.e. O/ N₂ ratio (Titheridge 1974). Also, for all seasons, pre-midnight values were higher than
313 post-midnight values as follows: In 2011, pre- and post-midnight values range from 8 – 30
314 TECU and 3 – 13 TECU respectively. In 2012, pre- and post-midnight values are in the range of
315 9 – 35 TECU and 3 – 17 TECU respectively. 2013 recorded pre-midnight values in the range 9 –
316 35 TECU and post-midnight values in the range 3 – 15 TECU. While, 2014 pre-midnight value
317 is between 9 and 47 TECU and its post-midnight range is 3 – 18 TECU.

318 Furthermore, the maximum OBS-TEC values and the corresponding annual range error
319 for all the seasons can be up to 49 TECU (September equinox) which is ~ 8m in 2011. 2012 and
320 2013 recorded annual range error of ~ 8m which corresponds to the maximum OBS-TEC value
321 of 52 TECU (September equinox) and 53 TECU (December solstice). While in 2014, maximum
322 OBS-TEC is 70 TECU (March equinox) which is approximately equals to 11m of delay.



323 Figure 10 shows the plot of annual variation of OBS-TEC and sunspot number, Rz
324 against the months of the year for the four years. The plots reveal the strong dependence of OBS-
325 TEC on solar activity (sunspot number). TEC and sunspot number increased gradually from
326 2011 to 2014. Although solar cycle 24 is regarded as a quiet solar cycle, which peaked in 2014,
327 the sun erupted with some few major flares in February and October of the same year (Kane,
328 2002). Hence, February, October and November 2014 were months of highest TEC values. An X-
329 class type solar flare was reported in February of 2011, resulting in a high value of sunspot
330 number. Increase in the sun's activities increases the number of electrons along the line of sight
331 (LOS) from a satellite to receiver on ground.



332

333 Figure 10: Annual variation of OBS-TEC and sunspot number, Rz during (a) 2011 (b) 2012 (c) 2013
and (d) 2014.

334 High solar activity produces solar flares of varying classes. As solar particles crash with
335 nitrogen and oxygen atoms in the upper atmosphere, these classes of flares produce waves of
336 ionization in the ionosphere that briefly alters the propagation of radio signals (Kane, 2002).
337 When solar flares become very intense, their electric field impulses, caused by disruption in the
338 earth's magnetic field due to ionization particles, may damage infrastructure such as power grids



339 and telephone lines not adequately protected against the geo-magnetically induced current (GIC),
340 leading to wastage of economic resources. Several earth-orbiting satellites may be in similar
341 danger. Hence, efforts are being made to develop tools and models from scientific results, to
342 forecast localised GIC impacts in national infrastructure. This forecasting capability will provide
343 operators with the information required to make swift operational decision, which may include
344 cancelling maintenance work or re-routing load in order to protect national infrastructure.
345 Operators will also advice when it is considered safe to resume normal operations.

346 CONCLUSIONS

347 Studies on OBS-TEC variations at Birnin-Kebbi in Northern Nigeria during the ascending and
348 maximum phases of solar cycle 24 have been carried out. The result obtained reveals the
349 following:

350 1. Higher TEC day-to-day variations during the daytime than nighttime for all the years
351 were observed. The diurnal variation shows OBS-TEC rising rapidly from a minimum
352 just before sunrise between 03:00 – 05:00 LT (~2 TECU) in 2011, 04:00 – 05 LT (~3
353 TECU) in 2012, 03:00 – 05:00 LT in 2013 (~3 TECU), and 03:00 – 05:00 LT in 2014 (~3
354 TECU). OBS-TEC is found to increase to a broad daytime maximum between 00:12 LT
355 – 00:16 LT for all years before falling to a minimum after sunset. While the diurnal
356 variation of IRI-2016 model shows TEC rising from a minimum of ~ 2 TECU in 2011, ~
357 4 TECU in 2012 and 2013, and ~ 5 TECU in 2014 between 03:00 – 04:00hr, to a broad
358 daytime peak between 08:00 – 14:00hr, before falling steeply to minimum before sunset
359 2. The diurnal variation reveals that the peak of OBS-TEC of some months were delayed till
360 after-noon. Post-sunset decrease and enhancement due to pre-reversal zonal electric field
361 after sunset, were also observed in the diurnal variation of TEC in some months.



362 3. On a general note, it can be concluded that IRI-2016 model did not predict well
363 throughout the day except during the post-midnight hours (00 – 04hr) in the NEI.
364 4. For all seasons, pre-midnight values were higher than post-midnight values. In 2011, pre-
365 and post-midnight values range from 8 – 30 TECU and 3 – 13 TECU respectively. In
366 2012, pre- and post-midnight values are in the range of 9 – 35 TECU and 3 – 17 TECU
367 respectively. 2013 recorded pre-midnight values in the range 9 – 35 TECU and post-
368 midnight values in the range 3 – 15 TECU. While, 2014 pre-midnight value is between 9
369 and 47 TECU and its post-midnight range is 3 – 18 TECU.
370 5. Maximum OBS-TEC values and the corresponding annual range error for all the seasons
371 recorded 49 TECU (~ 8m) in 2011. 2012 and 2013 also recorded annual range error of ~
372 8m corresponding to the maximum GPS-TEC value of 52 TECU and 53 TECU
373 respectively. While in 2014, maximum GPS-TEC is 70 TECU which is approximately
374 equals to 11m of delay.
375 6. Finally, annual variation of OBS-TEC and sunspot number, Rz against the months of the
376 year for the four years were plotted. The plots reveal the strong dependence of TEC on
377 solar activity (sunspot number). OBS-TEC and sunspot number were found to increase
378 gradually from 2011 to 2014.

379

380 **ACKNOWLEDGEMENT**

381 We thank the Office of the Surveyor General of the Federation (OSGoF) for making TEC data
382 available through the infrastructure www.nignet.net. We also thank Hatanaka, Y., Gopi Krishna
383 for providing TEC processing software online. Finally, we appreciate Bilitza *et al.* (2017) for
384 making the latest version of IRI model available online.



385 **REFERENCES**

386 Aggarwal, M., Bardhan, A., Sharma, D.K. Equinoctial asymmetry in ionosphere over Indian
387 region during 2006 – 2013 using COSMIC measurements. *Advances in Space Res.*, 60, 999 –
388 1014, 2017.

389 Akala, A.O., Somoye, E.O, Adeloye, A.B., Rabiu, A.B. Ionospheric f_0F_2 variability at equatorial
390 and low latitudes during high, moderate and low solar activity. *Indian Journal of Radio and*
391 *Space Physics*. Vol. 40, pp 124 – 129, 2011.

392 Akala, A.O., Seemala, G.K., Doherty, P.H., Valladares, C.E., Carrano, C.S., Espinoza, J., and
393 Oluyo, K.S. Comparison of equatorial GPS-TEC observations over an African station and an
394 American station during the minimum and ascending phases of solar cycle 24. *Ann. Geophys.*,
395 31, 2085, 2013.

396 Alizadeh, M.M., Wijaya, D.D., Hobiger, T., Weber, R., Schuh, H. Ionospheric effects on
397 microwave signals in J. Bohm and H. Schuh (eds). *Atmospheric Effect in Space Geodesy*.
398 Springer atmospheric sciences. Doi: 10.1007/978-3-642-36932-2_2, © Springer-Verlag Berlin
399 Heidelberg, 2013.

400 Ayorinde, T.T., Rabiu, A.B., and Amory-Mazaudier, C. Inter-hourly variability of Total Electron
401 Content during the quiet condition over Nigeria within the Equatorial Ionization Anomaly
402 region. *J. Atmos. Solar Terr. Phys.*, 145, 21 – 33, 2016.

403 Bagiya, M.S., Joshi, H.P., Iyer, K.N., Aggarwal, M., Ravin-dran, S., and Pathan, B.M. TEC
404 variations during low solar activity period (2005 – 2007) near the Equatorial Ionization Anomaly
405 Crest region in India. *Ann Geophys.*, 27, 1047 – 1057, 2009.



406 Bhuyan, P.K. and Borah, R.R. TEC derived from GPS network in India and comparison with the
407 IRI. *Advances in Space Res.*, 39, 830 – 840, 2007.

408 Bilitza, D., Altadill, D., Zhang, Y., Mertens, C., Truhlik, V., Richards, P., McKinnell, L.A.,
409 Reinisch, B. International reference ionosphere 2012 – A model of international collaboration. *J.*
410 *Space Weather Space Clim.*, 4, 1 – 12, doi: 10.1002/201JA018009, 2014.

411 Bilitza, D., Altadill, D., Truhlik, V., Shubin, V., Galkin, I., Reinisch, B., and Huang, X.
412 International reference ionosphere 2016: from ionospheric climate to real-time weather
413 predictions. *Space weather*, 15, 418 – 429, doi: 10.1002/2016SW001593, 2016.

414 Bolaji, O. S., Adeniyi, J.O., Radicella, S.M., and Doherty, P.H. Variability of total electron
415 content over an equatorial West African station during low solar activity. *Radio Sci.*, 47,
416 RS1001, doi: 10.1029/2011RS004812, 2012.

417 Ciraolo, L., and Spalla, P. TEC analysis of IRI simulated data. *Adv. Space Res.*, 29, 6, 959 –
418 966, 2002.

419 Dabas, R.S., Singh, L., Lakshmi, D.R., Subramanyam, P., Chopra, P., Garg, S.C. Evolution and
420 dynamics of equatorial plasma bubbles: relationships to $\mathbf{E} \times \mathbf{B}$ drifts, post-sunset total electron
421 content enhancements, and equatorial electrojet strength. *Radio Sci.*, 38, doi:
422 10.1029/2001RS002586, 2003.

423 D'ujanga, F.M., Opio, P. Twinomugisha, F. Variation of total electron content with solar activity
424 during the ascending phase of solar cycle 24 observed at Makerere University, Kampala. *Space*
425 *Weather: Longitude and Hemispheric Dependences and Lower Atmosphere Forcing*,
426 *Geophysical Monograph* 220, First Edition. Edited by Timothy Fuller-Rowell, Endawoke



427 Yizengaw, Patricia H. Doherty, and Sunanda Basu. © 2017 American Geophysical Union.

428 Published 2017 by John Wiley & Sons, Inc., 2017.

429 Eyelade, V.A., Adewale, A.O., Akala, A.O., Bolaji, O.S. and Rabiu, A.B. Studying the
430 variability in the diurnal and seasonal variations in GPS TEC over Nigeria. Ann. Geophys., 35,
431 701 – 710, 2017.

432 Fayose, R.S., Rabiu, B., Oladosu, O., Groves, K. Variation of total electron content (TEC) and
433 their effect on GNSS over Akure. Nigeria, Applied Physics Research, vol 4, No. 2, 2012.

434 Hajra, R., Chakraborty, S.K., Tsurutani, B.T., DasGupta, A., Echer, E., Brum, C.G.M.,
435 Gonzalez, W.D., Sobral, H.A. An empirical model of ionospheric total electron content (TEC)
436 near the crest of the equatorial ionization anomaly (EIA). J. Space Weather Space Clim., 6, A29,
437 doi: 10.1051/swsc/2016023, 2016.

438 Kane, R.P. Some implications using the group sunspot number reconstruction. Solar Phys., 205,
439 2, 383 – 401, 2002.

440 Okoh, D., Lee-Anne McKinnell, L., Cilliers, P., Okere, B., Okonkwo, C., Rabiu, A.B. IRI-VTEC
441 versus GPS-vTEC for Nigerian SCINDA GPS stations. Advances in Space Research,
442 <http://dx.doi.org/10.1016/j.asr.2014.06.037>, 2014.

443 Ogunmodimu, O., Rogers, N.C., Falayi, E., Bolaji, S. Solar Flare induced cosmic noise
444 absorption, NRIAG Journal of Astronomy and Geophysics. 7, 1, 31-39, 2018.

445



446 Ogwala, A., Somoye, E.O., Oyedokun, O., Adeniji-Adele, R.A., Onori, E.O., Ogungbe, A.S.,
447 Ogabi, C.O., Adejo, O., Oluyo, K.S., Sode, A.T. Analyses of Total Electron Content over
448 Northern and Southern Nigeria. *J. Res. and Review in Sci.*, 21 – 27, 2018.

449 Onwumechilli, C.A., and Ogbuehi, P.O. *Journal Atmos. Terr. Phys.*, 26, 894, 1964.

450 Rama Rao, P.V.S., Krishna, S.G., Prasad, J.V., Prasad, S.N.V.S., Prasad, D.S.V.V.D., Niranjan,
451 K. Geomagnetic storm effects on GPS based navigation. *Ann. Geophys.*, 27, 2101 – 2110, 2009.

452 Rama Rao, P.V.S., Krishna, S.G., Niranjan, K., Prasad, D.S.V.V.D. Study of temporal and spatial
453 characteristics of L-band scintillation over the Indian low-latitude region and their possible
454 effects on GPS navigation. *Ann. Geophys.*, 24, 1567 – 1580, 2006a.

455 Rama Rao, P.V.S., Krishna, S.G., Niranjan, K., Prasad, D.S.V.V.D. Temporal and spatial
456 variations in TEC using simultaneous measurements from Indian GPS network of receivers
457 during low solar activity period of 2004 – 2005. *Ann. Geophys.*, 24, 3279 – 3292, 2006b.

458 Rama Rao, P.V.S., Niranjan, K., Prasad, D.S.V.V.D., Krishna, S.G., Uma, G. On the validity of
459 the ionospheric pierce point (IPP) altitude of 350km in the Indian equatorial and low-latitude
460 sector. *Ann. Geophys.*, 24, 2159 – 2168, 2006c.

461 Suranya, P.L., Prasad, D.S.V.V.D., Niranjan, K., Rama Rao, P.S.V. Short term variability in
462 foF2 and TEC over low latitude stations in the Indian sector. *Indian J. of Radio and Space Phys.*,
463 44, 14 – 27, 2015.

464 Somoye, E.O. Diurnal and seasonal variation of fading rates of E- and F-region echoes during
465 IGY and IQSY at the equatorial station of Ibadan. *Indian Journal of Radio and space Physics*, 38,
466 194 – 202, 2010.



467 Somoye, E.O., Akala, A.O., Ogwala, A. Day-to-day variability of h'F and foF2 during some
468 solar cycle epochs. *Journal Atmos. Solar Terr. Physics*, 73, 1915 – 1922, 2011.

469 Tariku, Y.A. Pattern of GPS-TEC variability over low-latitude regions (African sector) during
470 the deep solar minimum (2008 to 2009) and solar maximum (2012 to 2013) phases. *Earth,*
471 *Planets, and space*. 67, 35, 2015.

472 Titheridge, J.E. Changes in atmospheric composition inferred from ionospheric production rates.
473 *J. Atmos. Terr. Phys.*, 36, 1249 – 1257, 1974.

474 Wu, C.C., Liou, K., Shan, S.J., Tseng, C.L. Variation of ionospheric total electron content in
475 Taiwan region of the equatorial anomaly from 1994 – 2003. *Adv. Space Res.*, 41, 611 – 616,
476 2008.

477

478